Magnetic and electronic properties of rhodium clusters

Chang-Hong Chien,[1] Estela Blaisten-Barojas,[1,*] and Mark R. Pederson[2]
[1]*Institute for Computational Sciences and Informatics, George Mason University, Fairfax, Virginia 22030*
[2]*Complex Systems Theory Branch, Naval Research Laboratory, Washington D.C. 20375-5320*
(Received 23 January 1998)

We have used all-electron local (LDA) and nonlocal (GGA) approximations to the density-functional theory to determine binding energies, equilibrium geometries, vibrational frequencies, and magnetic properties of Rh_N clusters ($N \leqslant 6$). We present careful tests on the Rh_2 dimer that compare results as calculated with a large (18-single Gaussian) and a very large (23-single Gaussian) basis sets. While the smaller set of Gaussians leads to underconverged results, we find that the large basis set leads to converged results that are also in excellent agreement with the experimental data available for Rh_2. The ground state of Rh_2 is confirmed to be a quintuplet, the trigonal Rh_3 is predicted to be a sextuplet, Rh_4 in its tetrahedral configuration is a singlet, Rh_5 sextuplet is a square pyramid, and Rh_6 septuplet is the octahedron. Results from several excited states are calculated and presented as well. It is found that LDA overestimates the binding energy but that GGA corrects this deficiency and predicts longer bond lengths.
[S1050-2947(98)12909-8]

PACS number(s): 36.40.Cg, 36.40.Mr, 61.46.+w

I. INTRODUCTION

The last decade has seen a considerable effort invested in the study of small clusters of heavy transition metals because of their application in catalysis and chemisorption processes. Rhodium is an interesting second-row transition metal because of its high melting point and relatively low mass density. It is used primarily as an alloying agent to harden platinum and palladium, and as a catalyst in a variety of hydrocarbon oxidation reactions. Experimental [1–5] and theoretical [6–15] investigations of rhodium clusters have been pursued by several authors. It is a challenge to the various theoretical calculations to represent correctly the electron correlation to accurately account for the large number of open-shell molecular electronic states that arise from incomplete filling of the $4d$ states of Rh. For Rh_2 through Rh_6 existing calculations are predominantly based on local-density approximation (LDA) theory. The LDA has some strengths and deficencies. Typically LDA yields accurate geometries [16–19], dipole moments [18], and vibrational frequencies [17–22]. On the other hand, atomization energies are overestimated [17,18,23,24]. Nonlocal schemes approximate the exchange-correlation energy by more sophisticated expressions that use gradients of the electronic density. For example, the generalized gradient approximation (GGA) successfully overcomes some of the LDA deficencies [23,25].

In this work we perform exhaustive all-electron LDA and GGA studies of Rh clusters containing up to six atoms. The ground state configuration of the Rh atom is a quartet [26,5]. Therefore, small rhodium clusters are expected to exhibit nonzero magnetic moments. On the other hand, bulk rhodium in its fcc phase is paramagnetic. In order to account properly for the magnetic properties, a precise calculation is required. In this work the electron density is obtained from a linear combination of localized atomic orbitals. We test the quality of several extended basis sets containing 18 and 23 primitive Gaussian functions and compare the ground-state energies and interatomic bond lengths resulting from the local to the nonlocal schemes. Vibrational and magnetic properties are calculated and compared with other calculations and with experiment. The energetics of Rh_2, Rh_3, Rh_4, Rh_5, and Rh_6 is described in subsections of Sec. II. Section III gives a discussion and several concluding remarks.

II. RHODIUM. THE ATOM AND SMALL CLUSTERS

The Kohn-Sham equations [27] were solved self-consistently using both the LDA and GGA representations of the exchange-correlation functionals. We use the PW91 local functional for the LDA calculations and the PW91 nonlocal functional for the nonlocal calculations [23]. Both LDA and GGA results give a ground state ^2D with spin configuration $[\mathrm{Kr}]4d_{\uparrow}^5 4d_{\downarrow}^4$ as shown in Table I. However, the ground state of atomic Rh is $^4F_{9/2}$ with configuration $[\mathrm{Kr}]4d^8 s^1$ [26]. The energy of these two states is close, 0.62 eV apart. We attribute this discrepancy to the limitations of the exchange-correlation representation.

A. Rh_2

The ground state of the rhodium dimer is ferromagnetic carrying a magnetic moment of $2\mu B$ per atom [1]. Previous calculations identified this state as a $^5\Sigma_g^+$ [6] and as a $^5\Delta_g$ [7,10] with leading electronic configuration $1\sigma_g^2, 2\sigma_g^2, \sigma_u^1, \delta_g^4, \delta_u^3, \pi_g^2, \pi_u^4$. Other calculations identified the ground state as $^5\Delta_u$ [8]. More recent calculations have assigned $^5\Sigma_u$ to the ground state [11,9]. We performed LDA and GGA calculations with spin multiplicity 5 and tested the quality of various basis sets of Gaussian functions. Sets $B1$ through $B3$ consist of 18 primitive functions whereas $B4$ is a larger set containing 23 primitives. The 18-exponent basis set consists of even-tempered exponents which range from 0.05 to 607 500. The 23-exponent basis set consists of expo-

*Electronic address: eblaiste@gmu.edu

TABLE I. Electronic configurations, atomic energies, and magnetic moments of the rhodium atom within LDA and GGA. Energies are relative to $E_{\mathrm{Rh}}=-127\,442.075$ eV for LDA and $E_{\mathrm{Rh}}=-127\,571.957$ eV for GGA.

Configuration	Energy (eV) LDA	GGA	Magnetic moment
$4d_{\uparrow}^{5}4d_{\downarrow}^{4}$	0	0	1
$5s_{\uparrow}^{1}4d_{\uparrow}^{5}4d_{\downarrow}^{3}$	0.719	0.622	3
$5s_{\uparrow}^{1}4d_{\uparrow}^{5}4d_{\downarrow}^{2}5p_{\uparrow}^{1}$	1.563	1.544	5
$5s_{\uparrow}^{1}4d_{\uparrow}^{5}4d_{\downarrow}^{1}5p_{\uparrow}^{2}$	14.502	13.991	7

nents between 0.043 065 69 and $1.377\,596\,6\times10^{7}$ but, rather than even tempering, each exponent has been adjusted to minimize the total energy of a spin unpolarized Rh atom [28]. From the 18-exponent basis set we develop three contracted sets $8s6p5d$, $11s9p8d$, and $12s10p9d$ ($B1-B3$) which include the atomic orbitals for the Rh atom plus diffuse Gaussian functions. For the 23-exponent basis set, the contraction $8s6p5d$ ($B4$) was adopted.

Table II and Fig. 1 summarize the calculated properties for the ground state. The various levels of approximation of the binding energies (dissociation energy) D_e as a function of interatomic bond length are illustrated in Fig. 1. Basis sets $B1$ through $B3$ show convergence as the atomic basis becomes larger. However, the best results are obtained with $B4$. Binding energies are referred to the energy of two Rh ^2D atoms at infinity calculated with the same basis set. There seems to be mixing of the atomic configurations ($4d^8 5s^1$) and ($4d^8$) in the dissociation pattern of Rh_2, making difficult the assignment of highly open shell states at long interatomic distances. As is apparent from our calculations, the quality of the calculation is strongly dependent on the basis set. A Morse function was fitted to our GGA calculation shown in Fig. 1 with a root mean square (rms) of 0.32 eV, equivalent to 11% error. A better fit to this functional is not possible. The Morse potential parameters resulting from the fit are $D_e=2.765$ eV, $r_e=2.331$ Å, and $\beta=1.641$. With the parameter β we can further estimate the anharmonic constant $\omega_e x_e=h\beta^2/8\pi c\mu=0.88\ \mathrm{cm}^{-1}$ where c is the speed of light and μ the reduced mass. The experimental binding energy is $D_e=2.92\pm0.22$ eV [1] from thermodynamic calculations with assumed values of $r_e=2.28$ eV and $\omega_e=267\ \mathrm{cm}^{-1}$. Recent experiments on mass selected Rh dimers in argon matrices [2] report a direct measure of $\omega_e=283.9\pm1.8\ \mathrm{cm}^{-1}$. These authors estimate a binding energy of $D_e=1.4\pm0.3$ eV from measurements of the anharmonicity constant $\omega_e x_e=1.48\ \mathrm{cm}^{-1}$. This estimate of the binding energy is, however, not accurate because the ground state is significantly distorted by the matrix effects. Therefore, to extrapolate the binding energy from the simple formula $D_e=\omega_e^2/4\omega_e x_e$ involves large errors at interatomic distances away from the minimum. The trend of our LDA calculations is to overestimate the binding energy, as shown in Table II. GGA corrects this effect favoring slightly larger bond lengths. Our GGA values are $D_e=2.765$ eV, $r_e=2.331$ eV, and $\omega_e=282\ \mathrm{cm}^{-1}$, which are in excellent agreement with

TABLE II. Binding energies D_e, bond lengths r_e, and vibrational frequencies ω_e of Rh_2 in its ground state with magnetic moment 2 μB/atom ($S=4$) within LDA and GGA.

	s	p	d	Method	r_3 (Å)	D_e (eV)	ω_e (cm^{-1})
$B1$	8	6	5	LDA	2.268	3.187	
$B2$	11	9	8	LDA	2.273	3.206	
$B3$	12	10	9	LDA	2.273	3.208	
$B4$	8	6	5	LDA	2.275	3.234	292
$B1$	8	6	5	GGA	2.313	2.683	
$B2$	11	9	8	GGA	2.317	2.698	
$B3$	12	10	9	GGA	2.316	2.626	
$B4$	8	6	5	GGA	2.331	2.765	282
Ref. [12]				GGA	2.26	3.03	
Ref. [11]				LDA	2.304		276
				GGA	2.564		191
Ref. [10]				LDA	2.31	3.04	333
Ref. [8]				CI	2.673	1.50	238
Ref. [7]				CI	2.28	2.10	266
Ref. [6]				CI	2.86	0.85	118
Ref. [1]				expt.	2.28	2.92 ± 0.22	267
Ref. [2]				expt.		1.4 ± 0.3	283.9 ± 1.8

experimental frequencies [2] and thermodynamic estimates of the binding energy [1]. Calculations by Yang, Toigo, and Wang within LDA [10] are comparable to our $B1$ results. Recently, Harada and Dexpert [11] reported LDA and GGA calculations that unfortunately cannot be fully compared to ours because total energies instead of binding energies are reported. Their calculated properties are $r_e=2.304$ Å, $\omega_e=276\ \mathrm{cm}^{-1}$ in LDA and $r_e=2.564$ Å, $\omega_e=191\ \mathrm{cm}^{-1}$ with the GGA correction. A few months ago, Nayak *et al.* [12] reported GGA results of $r_e=2.26$ Å and $D_e=3.03$ eV without a calculation of ω_e. We believe that the discrepancy of the bond distances and frequencies in Ref. [11] with our values and those in [12] is in the use of a different nonlocal correction and a less balanced basis set.

B. Rh_3

Matrix aggregation reactions of Rh atoms to form very small clusters have identified Rh_3 by UV absorption spec-

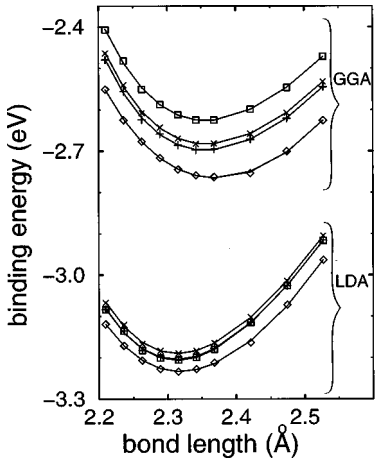

FIG. 1. Binding energy as a function of interatomic distance for the ground state ($S=4$) of Rh_2.

TABLE III. Binding energies E_b, bond lengths r_e, and normal mode frequencies ω of Rh_3 within LDA and GGA. For the isosceles triangle the second distance is the base of the triangle.

	Geometry	Spin	r_e (Å)	E_b (eV)	ω (cm^{-1})	$\epsilon_H^{\uparrow}$	$\Delta^{\uparrow}$	$\epsilon_H^{\downarrow}$	$\Delta^{\downarrow}$
LDA	Linear chain	1/2	2.197	6.174		4.649	0.000	4.790	0.438
	Equilateral triangle	3/2	2.382	7.147	322,199[a]	5.023	0.599	4.602	0.127
		5/2	2.430	7.013		4.560	1.670	4.569	0.000
		7/2	2.468	5.050		3.592	0.000	5.691	0.000
	Isosceles triangle	3/2	2.391,2.387	7.094	314,200,199	5.035	0.597	4.615	0.144
		5/2	2.441,2.436	6.962		4.560	1.704	4.579	0.000
		7/2	2.865,2.301	5.300		3.657	0.000	5.700	0.009
GGA	Linear chain	1/2	2.244	4.752		4.589	0.000	4.621	0.417
	Equilateral triangle	3/2	2.440	5.750	286,135[a]	4.968	0.482	4.528	0.266
		5/2	2.485	5.751		4.606	1.866	4.355	0.000
		7/2	2.485	4.073		3.440	0.000	5.341	0.017
	Isosceles triangle	3/2	2.419,2.419	5.832	290,139[a]	4.866	0.422	4.536	0.359
		5/2	2.637,2.438	5.857	269,167,125	4.617	1.863	4.328	0.122
		7/2	3.087,2.391	4.315		3.545	0.482	5.278	0.321
Ref. [10]	Linear chain	1/2	2.20	5.74					
	Equilateral triangle	3/2	2.42	6.76					
	Isosceles triangle	3/2	2.46,2.34	6.78					
Ref. [12]	Equilateral triangle	3/2	2.49	5.97					
Ref. [13]	Isosceles triangle	3/2	2.535,2.596	8.150					
Ref. [14]	Isosceles triangle	5/2	2.612,2.241	10.754					

[a]Double degenerate mode.

trometry in Ar solid matrices [29]. The trimer has also been observed in mass spectra [3,4]. The electron-spin resonance spectra [5] reveal that Rh_3 probably has total magnetic moments 5 and 7 μB. Early *ab initio* investigations by Das and Balasubramanian [13] report eight doublet and quartet states in the C_{2v} symmetry bundled within an energy separation of 0.2 eV. More recently, extensive CI calculations [14] identify several states with multiplicity 6 and 8 within the C_{2v} confirming that $^6A_1$ is the ground state. However, recent LDA results [10] identify a C_{2v} quartet as the ground state.

Our LDA and GGA calculations were both carried out with the $B4$ basis set. There is only one other calculation within the GGA approach for Rh_3 [12]. Tables III and IV summarize our results for the $D_{\infty h}$ (linear chain), C_{3v} (equilateral triangle), and C_{2v} (isosceles triangle) symmetries. Table III shows the geometries, binding energies, normal mode vibrational frequencies, energies of the highest occupied molecular orbital (HOMO) (ϵ_H) with spin up and down, and the energy gap Δ between the HOMO and LUMO of one-electron states associated to spin up and down calculated at the equilibrium configuration. The binding energies were calculated with respect to the energy of three Rh ^2D atoms at infinity. The lowest-energy state of the trimer is found to correspond to the isosceles triangle with $S=5/2$. Our best geometry in the C_{2v} symmetry has interatomic lengths 2.637 and 2.438 Å, comparable to the CI results 2.612 and 2.241 Å [14]. On the other hand, a marked discrepancy exists between the CI calculation of the binding energy 10.794 eV [14] and our result of 5.857 eV.

Both the C_{2v} and C_{3v} symmetries exhibit a higher-energy state with $S=3/2$. However, in the GGA approximation the $S=3/2$ C_{2v} state relaxes to the C_{3v} symmetry at the equilibrium configuration. This relaxation effect must have been observed in Ref. [12], where the quartet C_{3v} was reported as the ground state. It is not clear whether Nayak *et al.* [12] searched for the sextuplet and found that under their nonlocal correction the quartet C_{3v} was more stable, or if they only searched multiplicities up to 4. For the linear chain the most stable state is a doublet.

Worth emphasizing is the importance of both the nonlocal correction and a well-balanced large basis set. These improvements over LDA permit us to predict that the sextuplet states for both C_{2v} and C_{3v} are more stable than the quartet states. LDA alone is not able to invert the ordering. In addition, we found that as a function of bond distance several states present a crossing of the HOMO and the LUMO ($\Delta=0$) at the equilibrium geometry. In those situations it is not possible to calculate the vibrational frequencies because of the accidental degeneracy. Thus, the frequency column in Table III corresponding to those states is empty. The calculation of the normal mode frequencies of Rh_3 are the first in the literature.

Table IV illustrates the changes in the binding energy as a function of bond length of the quartet and sextuplet states for the C_{2v} configuration. As is apparent, the GGA correction enlarges the bond lengths and decreases the binding energy. It is worthwhile noting that the GGA reduces the curvature of the energy function, which leads to a softening of the vibrational frequencies. This is in accord with the general trend that has been observed in all atomic systems that are devoid of hydrogen. For a discussion of this see Ref. [30] and references therein. The last column of Table IV indicates the energy difference between the HOMO and the LUMO states of spins up or down:

$$\delta\epsilon=\epsilon_L^{\uparrow}-\epsilon_H^{\downarrow} \quad \text{for } S=3/2, \quad \delta\epsilon=\epsilon_L^{\downarrow}-\epsilon_H^{\uparrow} \quad \text{for } S=5/2. \tag{1}$$

TABLE IV. Total energies E_b relative to the ground state of Rh_3 in the C_{2v} configuration with bond lengths r_1, r_2. The last column is the energy difference of Eq. (1).

	Spin	r_1 (Å)	r_2 (Å)	Angle	E_b (eV)	$\delta\epsilon$ (eV)
GGA	3/2	2.419	2.419	59.998	5.833	0.245
		2.384	2.439	61.552	5.816	0.228
		2.479	2.386	57.529	5.807	0.223
		2.489	2.389	57.362	5.806	0.212
		2.492	2.390	57.314	5.806	0.209
		2.637	2.438	55.069	5.713	0.082
	5/2	2.637	2.438	55.069	5.857	0.411
		2.648	2.445	54.979	5.856	0.425
		2.620	2.452	55.809	5.854	0.392
		2.503	2.486	59.572	5.794	0.250
		2.506	2.489	59.553	5.793	0.252
		2.522	2.501	59.447	5.792	0.275
		2.809	2.404	50.680	5.784	0.506
		2.649	2.358	52.868	5.780	0.415
		2.437	2.438	60.010	5.758	0.152
		2.561	2.530	59.204	5.720	0.397
LDA	3/2	2.391	2.387	59.905	7.094	
		2.353	2.386	60.918	7.085	
		2.463	2.344	56.827	7.058	
		2.461	2.343	56.853	7.057	
		2.493	2.360	56.508	7.046	
		2.478	2.476	59.955	6.957	
		2.637	2.438	55.069	6.829	
		2.260	2.235	59.273	6.613	
	5/2	2.441	2.436	59.890	6.962	
		2.425	2.425	60.001	6.960	
		2.443	2.438	59.874	6.949	
		2.548	2.517	59.179	6.842	

When the geometry is the same for both the quartet and sextuplet states, the quartet GGA total energy is 0.144 eV higher than the sextuplet total energy. On the other hand, the small $\delta\epsilon = 0.082$ eV suggests that when this energy is available a flip of the minority spin will induce a transition from the quartet to the sextuplet. However, a transition from the sextuplet to the quartet requires about twice as much energy.

C. Rh_4

There are experimental indications that most of the small Rh clusters exhibit nonzero magnetic moments [3,4]. For example, Rh_{13} exhibits 0.48 μB/atom. It is therefore possible that under certain conditions Rh_4 would be magnetic. Previous LDA calculations [10] indicate that the ground state T_d of the tetramer is paramagnetic. The C_{3v} lower-energy state is also paramagnetic, and two higher-energy states with $S = 2$ were identified for the D_{4h} and D_{2h} symmetries.

Table V and Fig. 2 summarize our results. We obtain a different ordering of states and symmetries than Yang, Toigo, and Wang [10] whereas our results agree with the findings of Nayak *et al.* [12]. The only three-dimensional geometry identified is the tetrahedron (T_d). This cluster is paramagnetic ($S = 0$). The trigonal pyramid C_{3v} is not stable and decays to the tetrahedron in both the LDA and GGA schemes. The most stable planar structure is the $S = 2$, D_{4h} (square) with magnetic moment of 0.5 μB/atom. The D_{2h} (rhombus) is not stable and decays to the square for $S < 4$. Binding energies of the magnetic states are about 0.2–0.4 eV above the paramagnetic ground state, and thus difficult to excite thermally at intermediate temperatures. However, it is not excluded that a transition from the nonmagnetic tetrahedron to the magnetic planar geometry would be induced under pressure. This might be the case when the tetramer is trapped in a solid matrix. The last four columns in Table V show the one-electron energy of the HOMO and the energy gap between the HOMO and the LUMO for states with spin up and down. As in the case of the trimer, some states exhibit the characteristic HOMO-LUMO crossing that disables the calculation of the vibrational frequencies.

Figure 2 illustrates the binding energy as a function of bond length for two paramagnetic states and several magnetic states of the tetrahedron and the square. Once again, the GGA calculation gives slightly longer bond lengths than LDA. The frequencies of the normal modes of vibration reported in Table V are new and constitute a theoretical prediction. It would be interesting to have experimental results for comparison.

D. Rh_5

Table VI contains the results obtained for this cluster size. The most stable structure is the square pyramid C_{4v} in the $S = 5/2$ state. This cluster is highly magnetic, suggesting the possibility that clusters with odd number of atoms would retain a magnetic characteristic. This result was obtained within both LDA and GGA. In this geometry, there is a bundle of states with different multiplicities very close in energy. The trigonal bipyramid D_{3h} most stable configuration is a quartet that lies above all the square pyramid states. Yang, Toigo, and Wang [10] report the $S = 3/2$ trigonal bipyramid as the ground state. In addition, in Table VI we report the normal mode frequencies for the square pyramid and the trigonal bipyramid. The calculation of these frequencies is a major computational effort. There are no measurements of these frequencies. It would be very interesting to have experimental numbers to compare with the predictions put forward in this paper.

E. Rh_6

For this cluster size we only studied the octahedron O_h in the GGA approximation. Spin states up to $S = 4$ were investigated, being the septuplet the most stable state. In LDA, Yang, Toigo, and Wang [10] reported that the octahedron is paramagnetic, which is contrary to our findings within GGA. This may be another example of a LDA deficiency that is improved by GGA. The binding energies obtained within GGA are -17.039, -16.810, -16.899, -17.294, and -17.180 eV corresponding to $S = 0$, 1, 2, 3, and 4, respectively. The bond length of the octahedron in these states is, respectively: 2.563, 2.575, 2.586, 2.598, and 2.622 Å. There is a clear trend to an expansion of the cluster as the total magnetic moment per atom increases.

III. CONCLUSION

In the study of rhodium clusters theoretical work on electron-spin magnetic ordering has taken the lead over the

TABLE V. Binding energy E_b, bond length r_e, and vibrational frequencies ω of Rh_4 within LDA and GGA. The second distance corresponds to the outer bond in the linear chain and to the base in the trigonal pyramid.

	Geometry	Spin	r_e (Å)	E_b (eV)	ω (cm^{-1})	$\epsilon_H^{\uparrow}$	$\Delta^{\uparrow}$	$\epsilon_H^{\downarrow}$	$\Delta^{\downarrow}$
LDA	Linear	1	2.245,2.183	8.793		4.755	0.020	5.257	0.000
	Square	0	2.326	11.179		4.271	0.007	4.271	0.007
		1	2.334	11.387		4.322	0.116	4.460	0.138
		2	2.341	11.717	277,263,239,[a]146,113	4.401	0.500	4.419	0.297
		3	2.350	11.124		3.887	0.543	4.344	0.000
		4	2.361	10.850		3.842	0.194	3.571	0.298
	Tetrahedron	0	2.443	11.988	343,330,[a]164[b]	4.395	0.540	4.395	0.540
		1	2.469	11.582		4.085	0.000	4.371	0.000
		2	2.494	11.394		4.295	0.000	4.371	0.000
		3	2.518	11.410		4.491	1.640	4.418	0.029
		4	2.529	9.720		3.421	0.000	5.240	0.000
GGA	Linear	1	2.307,2.307	6.706		4.163	0.000	4.567	0.000
	Square	0	2.381	8.824		4.155	0.006	4.155	0.006
		1	2.391	9.129		4.240	0.220	4.171	0.249
		2	2.392	9.481	268,254,241,[b]159,101	4.318	0.587	4.161	0.275
		3	2.478	9.194		3.960	0.809	4.117	0.138
		4	2.494	8.036		3.678	0.000	4.991	0.147
	Tetrahedron	0	2.500	9.679	309,207,[a]135[b]	4.246	0.583	4.246	0.583
		1	2.525	9.276		3.932	0.000	4.173	0.000
		2	2.550	9.177		4.187	0.000	4.128	0.000
		3	2.576	9.360		4.425	1.778	4.139	0.031
		4	2.591	7.828		3.213	0.000	4.867	0.000
Ref. [10]	Linear chain	1	2.22	8.22					
	Square	2	2.41	10.91					
	Rhombus	2	2.39	10.93					
	Tetrahedron	0	2.48	11.80					
	Trigonal pyramid	0	2.45,2.42	11.79					
Ref. [12]	Square	2	2.38	9.4					
	Tetrahedron	0	2.42	9.64					

[a]Triple degenerate mode.
[b]Double degenerate mode.

progress in the experimental front. Extensive calculations have been made for rhodium to understand the collective properties of their electron spins. These studies are also relevant outside the field of spin magnetism since the spin assemblies in metals are good realizations of several widely investigated model systems.

Motivated by the richness of the possible closed and opened spin configurations in rhodium, most of our work has concentrated on determining the magnetically ordered spin structures in this transition metal. It was found that different magnetic orders can coexist at room temperature for Rh_3, Rh_5, and Rh_6, (see Tables III and VI) whereas on the order of 2000 K would be necessary to promote Rh_4 from a paramagnetic to a magnetic state (Table V). Prediction of the vibrational frequencies for the trimer, tetramer, and pentamer should encourage experimentalists to verify these predictions. In the case of the dimer, our frequency calculation perfectly agrees with the most recent experimental measurements. The ability to determine Rh-cluster vibrational fre-

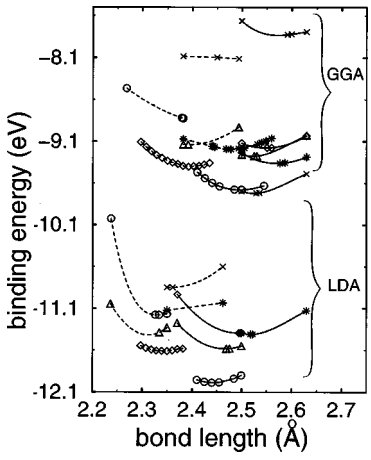

FIG. 2. Binding energy as a function of interatomic distance for Rh_4: $S=0$ (circles), $S=1$ (triangles), $S=2$ (diamonds), $S=3$ (asterisk), $S=4$ (crosses); T_d (solid lines), D_{4h} (dashed lines).

TABLE VI. Binding energy E_b, bond length r_e, and vibrational frequencies ω of Rh_5 within LDA and GGA. For the square pyramid the first distance corresponds to the side of the base and the second one is the side to the pyramid top. For the trigonal bipyramid, the first distance represents the side of the shared equilateral triangle and the second distance corresponds to the other sides.

	Geometry	Spin	r_e (Å)	E_b (eV)	ω_e (cm^{-1})	$\epsilon_H^{\uparrow}$	$\Delta^{\uparrow}$	$\epsilon_H^{\downarrow}$	$\Delta^{\downarrow}$
LDA	Square pyramid	1/2	2.540,2.405	16.351		3.400	0.003	4.072	0.296
		3/2	2.541,2.394	16.499		4.078	0.295	3.826	0.010
		5/2	2.559,2.403	16.537	294,219,[a]211, 190,153,147,[a]106	3.928	0.004	4.135	0.338
		7/2	2.591,2.423	16.387		3.989	0.698	4.203	0.117
	Trigonal bipyramid	1/2	2.484,2.845	16.153		4.235	0.386	3.929	0.024
		3/2	2.489,2.857	16.313		4.107	0.158	4.304	0.476
		5/2	2.506,2.861	16.010		4.100	0.000	4.208	0.000
		7/2	2.506,2.861	16.019		4.198	0.671	4.284	0.162
GGA	Square pyramid	1/2	2.594,2.459	13.171		3.827	0.069	3.843	0.378
		3/2	2.591,2.459	13.356		3.960	0.321	3.740	0.163
		5/2	2.653,2.435	13.494	275,197,190,[a] 169,133,[b]132,97	3.743	0.734	3.767	0.397
		7/2	2.663,2.478	13.474		3.933	0.865	4.012	0.227
	Trigonal bipyramid	1/2	2.549,2.934	12.931		4.135	0.493	3.802	0.152
		3/2	2.547,2.928	13.087	268,198,166[a] 146,136,[a]102[a]	4.007	0.246	4.063	0.514
		5/2	2.550,2.929	12.939		3.926	0.000	3.931	0.000
		7/2	2.562,2.930	13.107		4.098	0.796	3.966	0.157
Ref. [10]	Trigonal bipyramid	3/2	2.52	15.31					

[a]Double degenerate mode.

quencies is important from several standpoints. First, accurate prediction of such properties gives experimentalists an alternative means for identifying and detecting the clusters in their measurements. Second, rhodium is used as a catalyst and a complete understanding of all the processes that impact catalysis relies in part on the ability to calculate vibrational frequencies.

ACKNOWLEDGMENTS

E.B.B. acknowledges the Institute for Computational Sciences and Informatics for supporting C.H.C. and for supplying the computing time used in this work. M.R.P. was supported in part by the ONR Georgia Tech Molecular Design Institute (Grant No. N00015-95-1-1116).

[1] K. A. Gingerich and D. L. Cocke, J. Chem. Soc. Chem. Commun. **1**, 536 (1972).
[2] H. Wang, H. Haouari, R. Craig, Y. Liu, J. R. Lombardi, and D. M. Lindsay, J. Chem. Phys. **106**, 2101 (1997).
[3] A. J. Cox, J. G. Louderback, and L. A. Bloomfield, Phys. Rev. Lett. **71**, 923 (1993).
[4] A. J. Cox, J. G. Louderback, S. E. Apsel, and L. A. Bloomfield, Phys. Rev. B **49**, 12 295 (1994).
[5] R. J. Van Zee, Y. M. Hamrick, S. Li, and W. Weltner, Jr., Chem. Phys. Lett. **195**, 214 (1992).
[6] I. Shim, Mat. Fys. Medd. K. Dan. Vidensk. Selsk. **41**, 147 (1985).
[7] K. Balasubramanian and D. W. Liao, J. Phys. Chem. **93**, 3989 (1989).
[8] F. Illas, J. Rubio, J. Cañellas, and J. M. Ricart, J. Chem. Phys. **93**, 2603 (1990).
[9] A. Goursot, I. Papai, and C. A. Daul, Int. J. Quantum Chem. **52**, 799 (1994).
[10] J. Yang, F. Toigo, and K. Wang, Phys. Rev. B **50**, 7915 (1994).
[11] M. Harada and H. Dexpert, C. R. Acad. Sci., Ser. IIb: Mec., Phys., Chim., Astron. **322**, 239 (1996).
[12] S. K. Nayak, S. E. Weber, P. Jena, K. Wildberger, R. Zeller, P. H. Dederichs, V. S. Stepanyuk, and W. Hergert, Phys. Rev. B **56**, 8849 (1997).
[13] K. K. Das and K. Balasubramanian, J. Chem. Phys. **93**, 625 (1990).
[14] D. Dai and K. Balasubramanian, Chem. Phys. Lett. **195**, 207 (1992).
[15] B. V. Reddy, S. N. Khanna, and B. I. Dunlap, Phys. Rev. Lett. **70**, 3323 (1993).
[16] M. R. Pederson, K. A. Jackson, and W. E. Pickett, Phys. Rev. B **44**, 3891 (1991).
[17] J. Andzelm and E. Wimmer, J. Chem. Phys. **96**, 1280 (1992).
[18] B. G. Johnson, P. M. W. Gill, and J. A. Pople, J. Chem. Phys. **98**, 5612 (1993).

[19] D. Porezag and M. R. Pederson, Phys. Rev. B **54**, 7830 (1996).
[20] N. C. Handy, P. E. Maslen, R. D. Amos, J. S. Andrews, C. W. Murray, and G. J. Laming, Chem. Phys. Lett. **197**, 506 (1992).
[21] A. A. Quong, M. R. Pederson, and J. L. Feldman, Solid State Commun. **87**, 535 (1993).
[22] X. Q. Wang, C. Z. Wang, and K. M. Ho, Phys. Rev. B **48**, 1884 (1993).
[23] J. P. Perdew, J. A. Chevary, S. H. Vosko, K. A. Jackson, M. R. Pederson, D. J. Singh, and C. Fiolhais, Phys. Rev. B **46**, 6671 (1992), and references therein.
[24] J. P. Perdew and A. Zunger, Phys. Rev. B **23**, 5048 (1981).
[25] J. P. Perdew, K. Burke, and M. Ernzerhof, Phys. Rev. Lett. **77**, 3865 (1996).
[26] C. E. Moore, *Atomic Energy Levels*, Natl. Bur. Stand. Circ. No. 467 (U.S. GPO, Washington, DC, 1971); Vol. III.
[27] W. Kohn and L. J. Sham, Phys. Rev. A **140**, 1133 (1965).
[28] D. Porezag, Ph.D. thesis, Technische Universität Chemnitz-Zwickau, 1997; Basis sets are available at http://archiv.tu-chemnitz.de/pub/1997/0025.
[29] G. A. Ozin and A. J. L. Hanlan, Inorg. Chem. **18**, 1781 (1979).
[30] D. C. Patton, D. V. Porezag, and M. R. Pederson, Phys. Rev. B **55**, 7454 (1997).